

Sensor and Simulation Notes

Note 346

5 October 1992

On the Low-Frequency Electric Dipole Moment
of Impulse Radiating antennas (IRAs)

D. V. Giri and S. Y. Chu
Pro-Tech, 3708 Mt. Diablo Boulevard, #215
Lafayette, CA 94549-3610

Abstract

One way to radiate an impulse-like waveform is to employ a TEM-fed paraboloidal reflector antenna. Various performance features of this antenna, such as prepulse, impulse amplitude, impulse width etc., have been analyzed in the past [1 to 8]. It has been observed that the low frequency or late-time performance of this form of an IRA is governed by the electric and magnetic dipole moments. A knowledge of these dipole moments helps in designing an optimal matching network to be inserted at the junction of the feed horn and the reflector. Evaluation of the electric dipole moment is addressed in this note and the magnetic dipole moment will be considered in a future note.

CLEARED
FOR PUBLIC RELEASE
PL/PA 10 NOV 92

PL 92-0777

Preface

This work is performed by Pro-Tech and sponsored by Phillips Laboratory, Kirtland AFB, NM under the Small Business Innovative Research (SBIR) program. The encouragement and guidance of Capt. L. Miner, Dr. Carl E. Baum, and Mr. William Prather of Phillips Laboratory is gratefully acknowledged. The authors are also thankful to Dr. Everett Farr of Farr Research, Albuquerque, NM for valuable discussions.

Contents

Section	Page
I. Introduction	3
II. Ideal Dipole Moments of the Feed Horn	5
III. Normalized Electric Dipole Moment of IRAs	8
IV. Summary and Future Work	16
References	17
	18

I. Introduction

One form of an IRA consists of a TEM horn-fed paraboloidal reflector antenna [1]. We can think of the radiated waveform in different time regimes as follows. First, there is a relatively low amplitude (negative) step associated with the spherical wave emanating from the feed apex. This is followed by a large, narrow reflector impulse (positive) for an observation point on the reflector axis. This narrow impulse is then followed by a complicated waveform, returning to zero level. The temporal behavior of the radiated waveform after the narrow impulse is strongly influenced by the choice of the terminating impedance Z_t at the junction of the TEM horn and the reflector antenna. It is also well known that the time-domain radiated waveform must have a zero area to ensure the absence of a dc component in the radiated spectrum.

A simple choice of $Z_t = Z_c \equiv$ characteristic impedance of the feed horn will help in combining the radiation at low frequencies from the electric and magnetic dipole moments. It is noted that the electric dipole moment \vec{p}_1 is produced by the terminating impedance consisting of $(Z_t/2)$ in each arm. On the other hand, the magnetic dipole moment \vec{m}_1 is produced by the current flow in a closed loop formed by the feed and the reflector. More sophisticated choice of Z_t in relation to Z_c will help in optimizing the late-time radiated waveform after the narrow impulse. A knowledge of \vec{p}_1 and \vec{m}_1 is desirable in the design of a matching network that represents Z_t . Specifically, we seek to numerically evaluate \vec{p}_1 and \vec{m}_1 and then require

$$c |\vec{p}_1| = |\vec{m}_1| \quad (1)$$

where c is the speed of light in vacuum. Such a balancing of the dipole moments, by a proper choice of Z_t results in combining their radiation and minimizing oscillatory behavior in the radiated waveform at late times.

When we evaluate \vec{p}_1 and \vec{m}_1 , it is certainly desirable to normalize them to some "ideal" dipole moments. Presenting the results with dimensionless parameters increases their utility. We have chosen as the normalizing dipole moments \vec{p}_0 and \vec{m}_0 . \vec{p}_0 is obtained in the absence of the reflector under conditions of constant voltage on the feed arms (electric), and $|\vec{m}_0|$ is equated to $c |\vec{p}_0|$. It is observed that \vec{m}_0 is not well defined since the "loop" of current is not closed for an independent calculation of \vec{m}_0 . However, this is not critical since \vec{m}_0 is used only for the purpose of normalization. We now define

$$f_p \equiv \text{reduction factor in electric dipole moment} = \frac{|\vec{p}_1|}{|\vec{p}_0|} \quad (2)$$

$$f_m \equiv \text{reduction factor in magnetic dipole moment} = \frac{|\vec{m}_1|}{|\vec{m}_0|} \quad (3)$$

These factors f_p and f_m will at most have a value of 1, since dipole moments are reduced by the presence of the reflector. In the electric case, the reflector antenna is at zero potential and has negative charge induced on it, resulting in a reduction of dipole moment (i.e., $|\vec{p}_1| \leq |\vec{p}_0|$). Similar arguments can be made to justify $|\vec{m}_1| \leq |\vec{m}_0|$.

Furthermore, since the normalizing dipole moments are simply related by

$$c |\vec{p}_0| = |\vec{m}_0| \quad (4)$$

so that

$$\delta = \frac{f_p}{f_m} = \frac{|\vec{p}_1|}{|\vec{p}_0|} \frac{|\vec{m}_0|}{|\vec{m}_1|} = \frac{c |\vec{p}_1|}{|\vec{m}_1|} \quad (5)$$

The objective then is to choose the terminating impedance Z_t that makes $\delta = 1$, for a given TEM characteristic impedance Z_c , or a given value of the geometric factor $f_g = (Z_c/Z_0)$. An interesting question is to determine if there is a special feed geometry (opening angle of the feed arms), for a prescribed feed impedance that makes $\delta = 1$. Such are the issues addressed in this note.

In section 2, we derive \vec{p}_0 and \vec{m}_0 , the idealized dipole moments. the reduction factor f_p for the electric dipole moment is evaluated in Section 3. In Section 4, the remaining work for a future note relating to \vec{m}_1 is outlined. The note is concluded with a list of references.

II. Ideal Dipole Moments of the Feed Horn

In this section, we are concerned with the "ideal" dipole moments of the feed horn \vec{p}_0 (electric) and \vec{m}_0 (magnetic). The electric dipole moment \vec{p}_0 is to be evaluated in the absence of the reflector antenna. The feed horn consisting of two triangular shaped plates is shown in figure 1 along with a system of cartesian coordinates (x, y, z) with its origin at the feed apex. We can now find the dipole moments.

A. Electric Dipole Moment \vec{p}_0

Let us assume that the top and bottom conductors are at a potential of $+V_0$ and $-V_0$ respectively. $y = 0$ is a symmetry plane and a reference conductor at zero potential may be placed on the plane $y = 0$. The horizontal and slant lengths of the feed horn are respectively l and l_s . ζ is a coordinate along the top conductor and 2β is the opening angle of the feed horn. We have

$$Z_c \equiv \text{TEM impedance of feed horn} = Z_0 f_g \quad (\Omega) \quad (6a)$$

$$Z_0 \equiv \text{characteristic impedance of free space} \quad (\Omega) \quad (6b)$$

$$f_g \equiv \text{geometric factor of the TEM horn} \quad (6c)$$

$$\zeta \equiv \text{coordinate along the slant length} \quad (6d)$$

$$C' \equiv \text{capacitance/unit slant length} = \frac{1}{cZ_c} = \frac{\epsilon_0}{f_g} \quad (F/m) \quad (6e)$$

$$c \equiv \text{speed of light in vacuum} \quad (m/s) \quad (6f)$$

$$C \equiv \text{total capacitance} = \frac{l_s}{cZ_c} = \frac{l_s \epsilon_0}{f_g} \quad (F) \quad (6g)$$

$$Q \equiv \text{total charge} = \frac{2V_0 l_s}{cZ_c} = \frac{2V_0 l_s \epsilon_0}{f_g} \quad (\text{coulombs}) \quad (6h)$$

$$\pm V_0 \equiv \text{voltage on top and bottom conductors} \quad (V) \quad (6i)$$

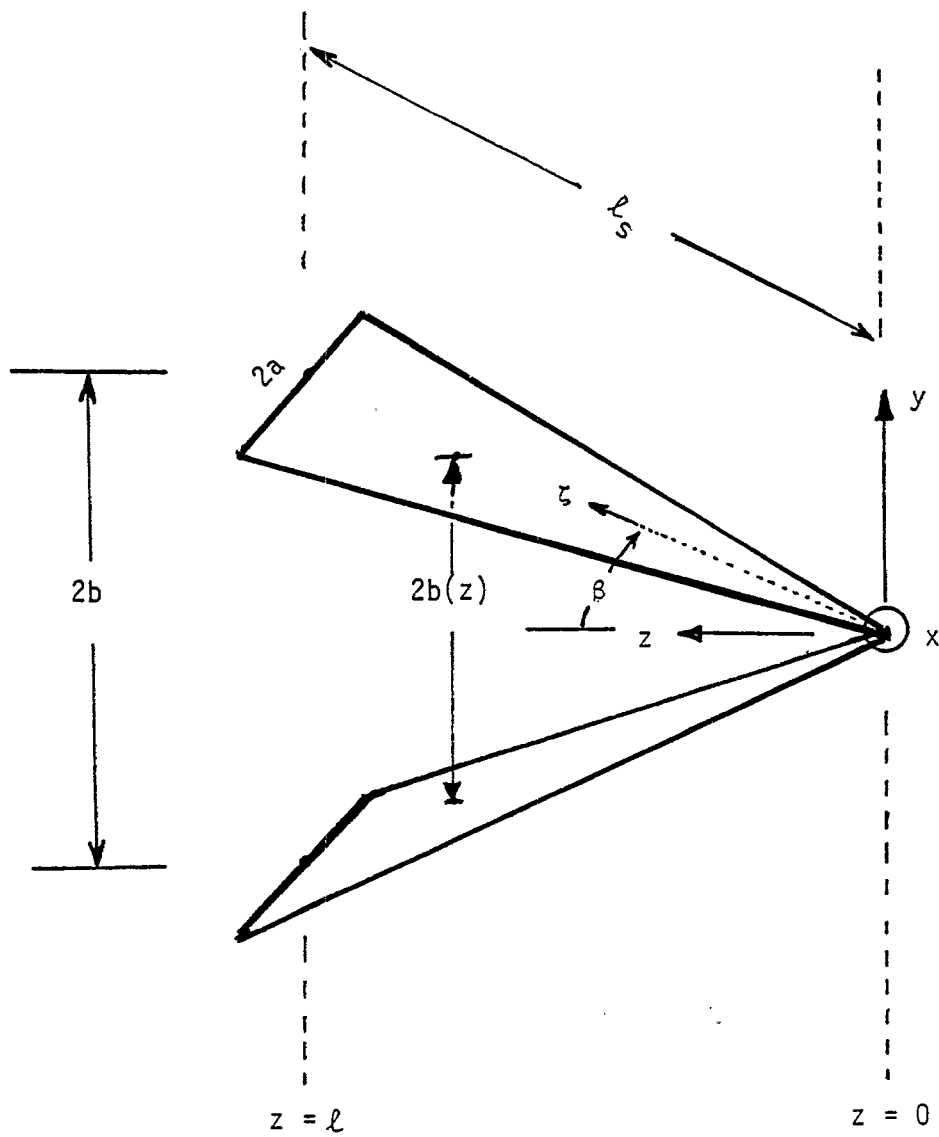


Figure 1. The feed horn

$$Q' \equiv \text{charge/unit slant length} = \frac{2V_0}{cZ_c} = \frac{2V_0\epsilon_0}{f_g} \quad (\text{coulombs/m}) \quad (6j)$$

We observe that in this idealized transmission-line model, the charge density Q' on the top conductor is a constant. The resulting electric dipole moment is given by

$$\vec{p}_0 = \vec{1}_y p_{oy} \quad (7)$$

$$p_{oy} = \int_0^{l_s} Q' [2b(z)] d\zeta$$

Substituting for $b(z) = z \tan(\beta) = \zeta \sin(\beta)$ and integrating, we have

$$\begin{aligned} p_{oy} &= Q' A_{eq} = Q' b l_s = Q' l_s^2 \sin(\beta) \\ &= Q h_{eff} = Q b \end{aligned} \quad (8)$$

We have introduced the equivalent area $A_{eq} [=l_s^2 \sin(\beta)]$ and an effective height $h_{eff} (=b)$ for the idealized electric dipole. Substituting for Q , we have,

$$p_{oy} = \frac{2V_0\epsilon_0}{f_g} b l_s \quad (9)$$

The dipole moment per unit voltage between the two conductors is obtained by setting $2V_0 = 1$ volt in (9).

As discussed above, we choose to define an idealized magnetic dipole moment \vec{m}_0 for normalization purposes only, as given by

$$\vec{m}_0 = \vec{1}_x m_{ox} \quad (10)$$

$$m_{ox} = c p_{oy} = 2V_0 \epsilon_0 \frac{c}{f_g} l_s^2 \sin(\beta) = \frac{2V_0}{Z_c} l_s^2 \sin(\beta) = I_0 l_s^2 \sin(\beta)$$

Once again the equivalent area of the idealized magnetic dipole moment \vec{m}_0 is $b l_s = l_s^2 \sin(\beta)$.

This completes the evaluation of the idealized electric (\vec{p}_0) and magnetic (\vec{m}_0) dipole moments used in normalizing the practical dipole moments \vec{p}_1 and \vec{m}_1 respectively.

III. Normalized Electric Dipole Moment of IRAs

In this section, we consider ways of evaluating \vec{p}_1 , the electric dipole moment of an IRA, as sketched in figure 2. Figure 2a shows the TEM feed with triangular shaped plates facing each other and in figure 2b, they are replaced by equivalent conical cylindrical rods. The equivalent rods of circular cross sections help in formulating the problem and in numerical computation of the electric dipole moment. The problem at hand may be posed as follows. With reference to figure 2b, the TEM feed is characterized at low frequencies by an electric potential of $\pm V_0$ on the two rods. We then seek the charge distribution on the feed conductors and the parabolic reflector, assuming an open-circuit at their junction. In the absence of the parabolic reflector, we observe that the electric charge distributes on the feed conductors in a certain fashion, resulting in a certain dipole moment. However, when the reflector is present, the charges redistribute in a manner that results in a lowered dipole moment.

The electrostatic problem of determining the charge distribution on the feed horn and the reflector, under the conditions of constant potential on the feed horn plates and open-circuit junction, may be solved via the Laplace differential equation for the potential or an integral equation for the charge distribution. In the method of Poisson's equation,

$$\left[\frac{\partial^2}{\partial x^2} + \frac{\partial^2}{\partial y^2} + \frac{\partial^2}{\partial z^2} \right] \phi(x, y, z) = - \frac{\rho}{\epsilon_0}(x, y, z) \quad (11)$$

one solves for the potential distribution $\phi(x, y, z)$ while noting that in charge free regions, the Poisson's equation reduces to Laplace's equation. $\phi(x, y, z)$ also satisfies the equipotential conditions on the feed horn, the image plane and the reflector surface. One then finds the normal electric fields on the metallic surfaces by taking the appropriate component of the negative gradient of the potential. The normal electric field on metal surfaces is relatable to the charge distribution. One can then find \vec{p}_1 , the electric dipole moment from the known charge distribution.

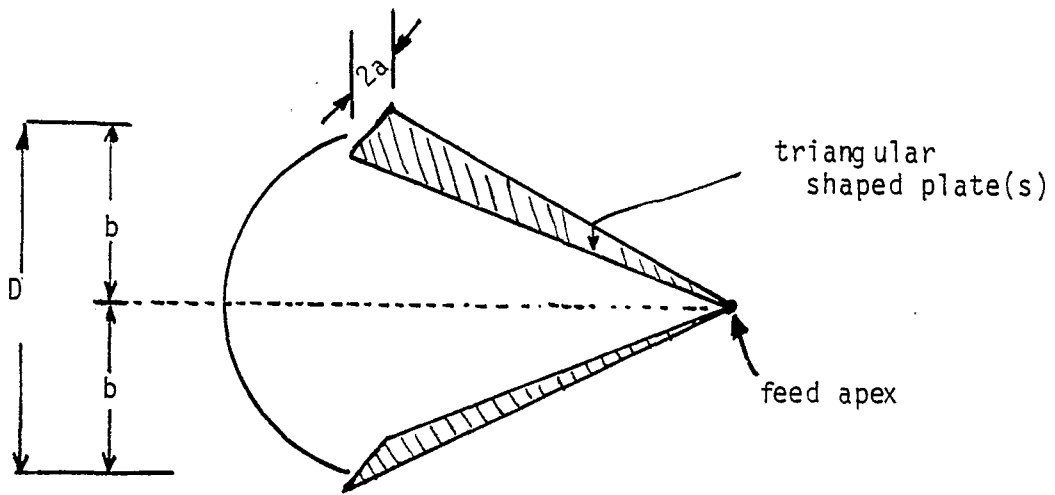
An alternate approach is to numerically solve for the electric charge distribution on conducting surfaces using an integral equation. Basically, by integrating the Poisson's equation above, one gets a complete solution for $\phi(x, y, z)$ as [9]

$$\phi(x, y, z) = \frac{1}{4\pi\epsilon} \int_V \frac{\rho}{R} dv + \frac{1}{4\pi} \int_S \left[\frac{1}{R} \frac{\partial\phi}{\partial n} - \phi \frac{\partial}{\partial n} \left[\frac{1}{R} \right] \right] dA \quad (12)$$

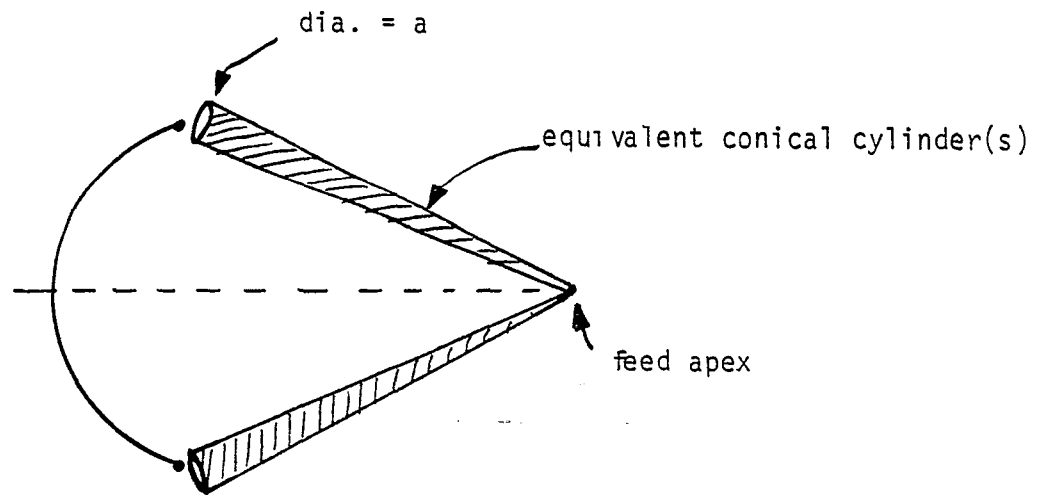
If the charges are distributed with a volume density $\rho(x, y, z)$ in a volume V bounded by a surface S and if there are no charges exterior to the surface S , the surface integral in (12) vanishes, resulting in the potential integral,

$$\phi(x, y, z) = \frac{1}{4\pi\epsilon} \iiint \frac{\rho(x', y', z')}{R} dv \quad (13)$$

with $R = (x-x')^2 + (y-y')^2 + (z-z')^2$



(a) feed horn consisting of triangular shaped plates



(b) feed horn consisting of equivalent conical conductors

Figure 2. Example of an IRA and the equivalent feed horn with conical cylinders

Equation (13) is a particular solution of the Poisson's equation valid at (x, y, z) . We have numerically solved the above integral equation satisfying the boundary conditions of

$$\begin{aligned}
 \phi &= V_o && \text{on the top feed arm} \\
 \phi &= -V_o && \text{on the lower feed arm} \\
 \phi &= 0 && \text{on the symmetry plane } y = 0 \\
 \phi &= 0 && \text{on the parabolic surface}
 \end{aligned}
 \tag{14}$$

A. Numerical Implementation

The potential integral (13) that uses volume density of charge may be cast in a form that uses surface density of charge. For example, we are modeling the feed horn plates by a conical conductor that is divided into N_1 number of elements. The volume integral becomes

$$\begin{aligned}
 \iiint \frac{\rho(x, y, z)}{R} dv &= \iint \rho_s(x, y, z) r d\theta d\zeta \\
 &= \int \rho_s(x, y, z) 2\pi r d\zeta
 \end{aligned}
 \tag{15}$$

where ρ_s is the surface density of charge (C/m^2). Similarly the paraboloidal surface is broken up into N_2 number of surface patches. We have developed computer routines that solve for the surface charge density in each of these segments along the feed conductors and each of these patches on the paraboloidal surface. A spherical coordinate system was defined at the feed apex to facilitate the numerical scheme. Once the surface charge densities are determined, a total charge Q_i (coulombs) can be assigned at the center of the segment or patch by a product of the surface charge density ρ_s and the area of the segment or patch. The electric dipole moment then is evaluated via

$$\vec{p}_1 = \sum_i Q_i y_i
 \tag{16}$$

As an example, if a typical surface patch along the paraboloidal surface extended from $(\theta_1$ to $\theta_2)$ and ϕ_1 to $(\phi_1 + \Delta\phi)$, the arc lengths are

$$\delta s_1 \equiv \text{arc length along } \theta = \frac{2\sqrt{2}f d\theta}{[1 + \cos(\theta)]^{3/2}}$$

$$\delta s_2 \equiv \text{arc length along } \phi = \frac{2f \sin(\theta) d\phi}{1 + \cos(\theta)}$$

$$dA \equiv \text{elemental area} = \frac{4\sqrt{2}f^2 \sin(\theta) d\theta d\phi}{[1 + \cos(\theta)]^{5/2}}$$

$$A_p \equiv \text{patch area} = \int_{\phi_1}^{(\phi_1 + \Delta\phi)} \int_{\theta_1}^{\theta_2} dA$$

$$= \frac{8}{3} \sqrt{2} f^2 \left\{ \left[\sec(\theta_2) \right]^{3/2} - \left[\sec(\theta_1) \right]^{3/2} \right\} \Delta\phi$$

where f is the focal length of the parabola. We experimented numerically with several types of patches, finally settling on nearly square ones. The symmetry plane at $y = 0$ is exploited and the computations are performed in one quadrant of the paraboloidal surface while accounting for the image plane and reflections. For any observation point, one has 6 contributions, i.e., upper arm, lower arm and the 4 quadrants of the paraboloidal surface. Similar integrals are used with appropriate sign changes to account for all contributions. In principle, this is a straight forward computation, but numerical convergence in the results was not trivial. Typically, we needed about 100 segments along the feed arm and about 1500 surface patches in one quadrant of the paraboloidal reflector.

B. Illustrative Results

For numerical purposes we have held the focal length $f = 1m$ or 1 unit of length. Summarizing the various parameters,

$$\begin{aligned} f &= 1 \text{ m} \\ d &= 1, 1.5, 2.0, 2.5 \text{ and } 3 \text{ m} \\ (f/D) &= 1, 0.667, 0.5, 0.4 \text{ and } 0.333 \\ 2b &= D \\ (b/a) &= 7 \quad (\text{fixed}) \end{aligned}$$

As the diameter of the dish D is varied, the plate separation $2b (=D)$ changes, as well as the feed angle β . However, the plate width $2a$ is varied so that (b/a) is held constant. Consequently, the characteristic impedance Z_c is held constant nominally at 400Ω .

A typical example of the charge distribution on the paraboloidal surface is shown in figure 3, for the case of

$$\begin{aligned} D &= 2.5 \text{ m}, & r &= D/2 = 1.25 \text{ m}, & f &= 1 \text{ m} \\ (f/D) &= 0.4, & 2b &= 2.5 \text{ m}, & 2a &= 0.36 \text{ m}, \\ (b/a) &\approx 7 & Z_c &\approx 400 \Omega. \end{aligned}$$

It is observed that the charge distribution on the paraboloidal surface is concentrated along the circular rim of the reflector, as well as near the junction between the feed arms and the

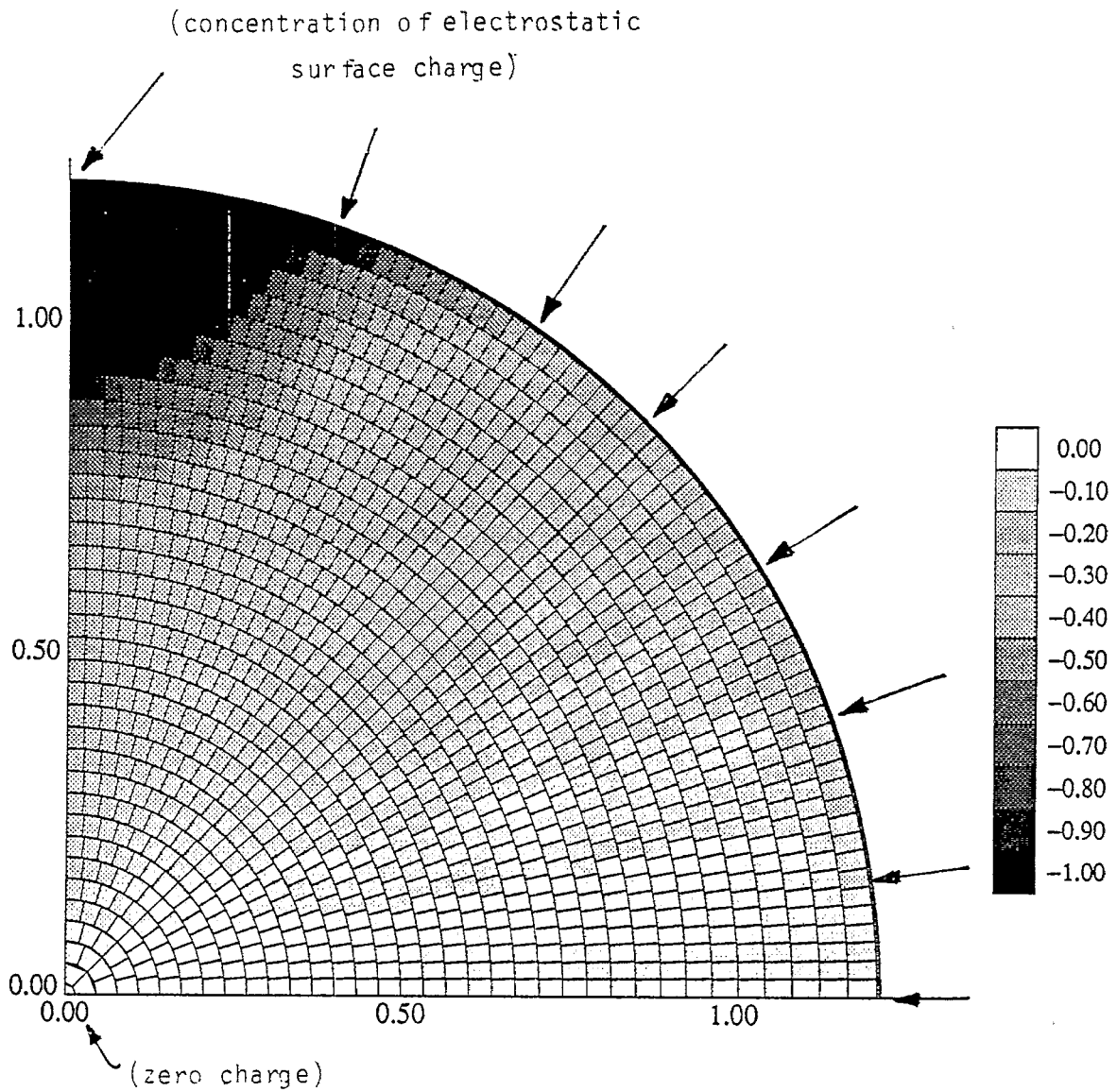


Figure 3. Surface charge distribution on one quadrant of the paraboloidal reflector (example case)

$$\begin{aligned}
 f = 1\text{m} & \quad ; \quad D = 2.5\text{m} & ; & \quad (f/D) = 0.4 \\
 2b = D = 2.5\text{m} & ; & 2a = 0.36\text{m} & ; & (b/a) = 7 \\
 Z_c = 400 \text{ Ohms} & & & &
 \end{aligned}$$

reflector. This is, as one would expect from physical considerations. The detailed zoning of one quadrant into roughly 1500 surface patches is also visible in figure 3.

The results of our numerical computations are presented in Table 1. The five cases correspond to (f/D) values ranging from 1 to 0.333. As the angle β is increased, keeping Z_c fixed, the reduction factor monotonically decreases. $\beta = 0$ corresponds to the case of no feed arm and $f_p = 1$ (no reduction in dipole moment). At $\beta = 90^\circ$, one would expect to have some "shielding" and hence f_p will have a finite non-zero value, as can also be seen in figure 4, where f_p is plotted as a function of β . In Table 1, the normalizing dipole moment $|\vec{p}_0|$ is also listed computed both analytically from (6) and (9) as well as through the computer routine by eliminating the parabolic reflector. The close agreement in $|\vec{p}_0|$ estimated by two methods enhances our confidence in the numerical procedure.

The remaining work consists of finding f_m , the corresponding reduction factor for the magnetic dipole moment reduction, to see if f_p can equal f_m which is a desirable condition for late-time radiated waveform characteristics.

Characteristic impedance of feed = 400 Ohms (nominal)

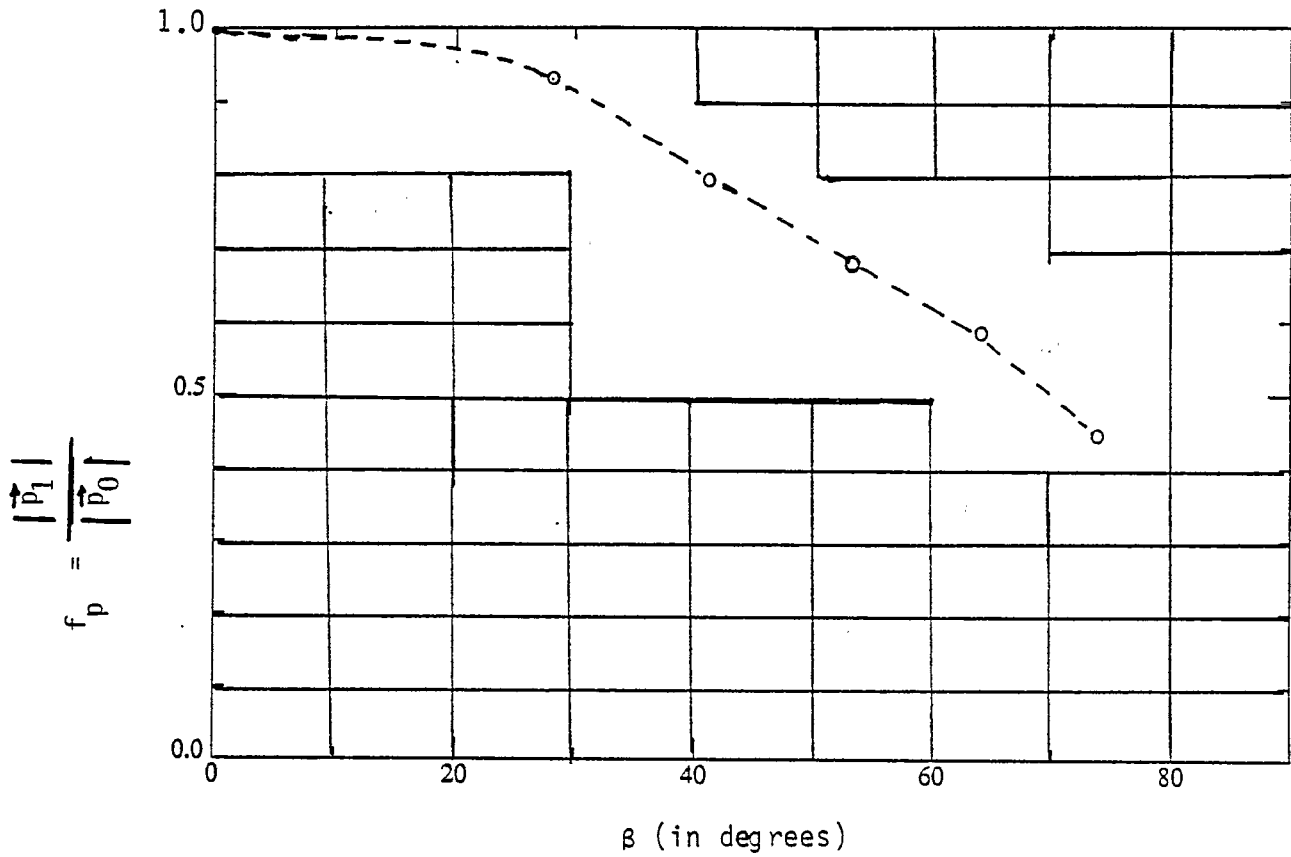


Figure 4. The normalized electric dipole moment of an IRA as a function of the feed angle β

NOTE: \vec{p}_1 \cong electric dipole moment with the reflector
 \vec{p}_0 \cong electric dipole moment without the reflector

IV. Summary and Future Work

In this note we have determined the electric dipole moment of an IRA for a set of parametric values of f/D , while holding the feed impedance nominally constant at 400Ω . What remains to be evaluated is the corresponding magnetic dipole moment. If the two dipole moments are related by the speed of light, the late-time behavior of the radiated waveform from the IRA is improved and better controlled. This is the goal of computations such as these. The problem of evaluating the magnetic dipole moment will be addressed in a future note.

References

- [1] C. E. Baum, Radiation of Impulse-Like Transient Fields, Sensor and Simulation Note 321, November 25, 1989.
- [2] C. E. Baum, Configurations of TEM Feed for an IRA, Sensor and Simulation Note 327, April 27, 1991.
- [3] C. E. Baum, Aperture Efficiencies for IRAs, Sensor and Simulation Note 328, June 24, 1991, and IEEE Antennas and Propagation Symposium, Chicago, July 1992.
- [4] E. G. Farr, Analysis of the Impulse Radiating Antenna, Sensor and Simulation Note 329, July 24, 1991.
- [5] C. E. Baum. General Properties of Antennas, Sensor and Simulation Note 330, July 23, 1991.
- [6] E. G. Farr and C. E. Baum, Prepulse Associated with the TEM Feed of an Impulse Radiating Antenna, Sensor and Simulation Note 337, March 1992.
- [7] E. G. Farr and C. E. Baum, A Simple Model of Small-Angle TEM Horns, Sensor and Simulation Note 340, May 1992.
- [8] E. G. Farr, Simple Models of Antennas Useful in Ultra-Wideband Applications, Transient Radiating Antenna Memos, Memo 2, July 1992.
- [9] J. A. Stratton, *Electromagnetic Theory*, McGraw Hill Book Company, 1941.